

Molecular Hydrogen in a Damped Lyman- α System at $z_{\text{abs}} = 4.224$ C. Ledoux¹, P. Petitjean^{2,3}, R. Srianand⁴**ABSTRACT**

We present the direct detection of molecular hydrogen at the highest redshift known today ($z_{\text{abs}} = 4.224$) in a Damped Lyman- α (DLA) system toward the quasar PSS J1443+2724. This absorber is remarkable for having one of the highest metallicities amongst DLA systems at $z_{\text{abs}} > 3$, with a measured iron abundance relative to Solar of -1.12 ± 0.10 . We provide for the first time in this system accurate measurements of N I, Mg II, S II and Ar I column densities. The sulfur and nitrogen abundances relative to Solar, -0.63 ± 0.10 and -1.38 ± 0.10 respectively, correspond exactly to the primary nitrogen production plateau. H₂ absorption lines are detected in four different rotational levels ($J = 0, 1, 2$ and 3) of the vibrational ground-state in three velocity components with total column densities of $\log N(\text{H}_2) = 17.67, 17.97, 17.48$ and 17.26 respectively. The $J = 4$ level is tentatively detected in the strongest component with $\log N(\text{H}_2) \sim 14$. The mean molecular fraction is $\log f = -2.38 \pm 0.13$, with $f = 2N(\text{H}_2)/(2N(\text{H}_2) + N(\text{H I}))$. We also measure $\log N(\text{HD})/N(\text{H}_2) < -4.2$. The excitation temperatures T_{01} for the two main components of the system are 96 and 136 K respectively. We argue that the absorbing galaxy, whose star-formation activity must have started at least $2 - 5 \times 10^8$ yrs before $z = 4.224$, is in a quiescent state at the time of observation. The density of the gas is small, $n_{\text{H}} \leq 50 \text{ cm}^{-3}$, and the temperature is of the order of $T \sim 90 - 180$ K. The high excitation of neutral carbon in one of the components can be explained if the temperature of the Cosmic Microwave Background Radiation has the value

¹European Southern Observatory, Alonso de Córdova 3107, Casilla 19001, Vitacura, Santiago, Chile; E-mail: cledoux@eso.org

²Institut d'Astrophysique de Paris – CNRS, 98bis Boulevard Arago, F-75014 Paris, France; E-mail: petitjean@iap.fr

³LERMA, Observatoire de Paris, 61 Avenue de l'Observatoire, F-75014, Paris, France

⁴IUCAA, Post Bag 4, Ganesh Khind, Pune 411 007, India; E-mail: anand@iucaa.ernet.in

expected at the absorber redshift, $T = 14.2$ K. These observations demonstrate the feasibility to study H_2 at the highest redshifts provided high enough spectral resolution and good S/N ratio are achieved.

Subject headings: cosmology: observations – galaxies: formation – ISM: molecules
– quasars: absorption lines

1. Introduction

Although molecular hydrogen, H_2 , is the most abundant molecule in the Universe, it is very difficult to detect directly. Emission lines from the tracer molecule CO are usually used instead but, at $z > 4$, only the brightest objects can be detected with current facilities (e.g., Omont et al. 1996; Solomon & Vanden Bout 2005). For the time being, the only way to detect H_2 directly at high redshift is to search for the absorption signature of the molecular UV transition lines from Damped Lyman- α (DLA) systems observed in the spectra of quasars or those of γ -ray burst afterglows.

DLA systems are characterized by very large neutral hydrogen column densities, $N(\text{HI}) \gtrsim 10^{20} \text{ cm}^{-2}$, that are typical of sightlines through local spiral galaxies. Inferred metallicities typically vary between $[\text{Zn,S}/\text{H}] = -2$ and -0.5 at $2 \lesssim z_{\text{abs}} \lesssim 3$ and are smaller at larger redshifts (e.g., Prochaska et al. 2003). The dust content is less than or about 10% of what is observed in the Galactic ISM for similar HI column densities (Ledoux et al. 2003). The detection of H_2 molecules in high-redshift DLA systems through Lyman-Werner band absorption is observationally challenging due to the presence of the Ly α forest. High spectral resolution, good S/N ratio and large wavelength coverage are simultaneously needed to detect the H_2 lines and avoid spurious detections (e.g., Levshakov & Varshalovich 1985; Ge & Bechtold 1999; Petitjean et al. 2000; Levshakov et al. 2002; Ledoux et al. 2002, 2003; Cui et al. 2005).

We are conducting a survey for molecular hydrogen in DLA systems at high redshift ($z_{\text{abs}} > 1.8$; see Ledoux et al. 2003), using the Ultraviolet and Visible Echelle Spectrograph (UVES; Dekker et al. 2000) at the European Southern Observatory’s Very Large Telescope, down to a detection limit of typically $N(\text{H}_2) = 2 \times 10^{14} \text{ cm}^{-2}$. Out of the 75 systems observed up to now, 14 have firm detections of associated H_2 absorption lines. In this Letter, we present the highest redshift detection in our sample, in the $z_{\text{abs}} = 4.224$ DLA system toward the quasar PSS J1443+2724. We describe the observations in Sect. 2 and the analysis of the data in Sect. 3. We conclude in Sect. 4.

2. Observations

The quasar PSS J1443+2724 ($z_{\text{em}} = 4.42$, $r \sim 19.3$) was observed with UVES in service mode on March 2-3 and 17-19, 2004. The red spectroscopic arm of UVES was used in the standard configuration with the central wavelength adjusted to 580 nm. The wavelength coverage was 478–681 nm with only a small gap, between 575 and 584 nm, corresponding to the physical gap between the two red arm CCDs. The CCD pixels were binned 2×2 and the slit width was fixed to $1''$, yielding, under the typical $0''.7$ seeing conditions achieved during the observations, a resolving power $R \approx 48000$. The total on-source integration time was 7.3 h, split into five exposures. The data were reduced using the UVES pipeline (Ballester et al. 2000) which is available as a dedicated context of the ESO MIDAS data reduction system. The wavelength scale of the spectra reduced by the pipeline was converted to vacuum-heliocentric values and individual exposures were scaled, weighted and combined altogether to produce the final object flux and variance spectra.

3. Analysis

3.1. The high metallicity and the star-formation history

The metallicity of the DLA system toward PSS J1443+2724 is the highest among the ten $z > 4$ DLA systems investigated up to now (Prochaska et al. 2003). Total integrated column densities and metallicities for N I, Mg II, S II, Ar I and Fe II, obtained from Voigt-profile fitting of the observed transition lines, are given in Table 1. With the exception of Fe II, these ions are observed here for the first time. We derive metallicities relative to Solar of $[\text{S}/\text{H}] = -0.63 \pm 0.10$ and $[\text{Fe}/\text{H}] = -1.12 \pm 0.10$. The latter value is consistent with the previous measurement by Prochaska et al. (2001) but we note that the newly determined H I and Fe II column densities are both larger by about 0.15 dex. Even though the depletion factor is moderate (i.e., $[\text{S}/\text{Fe}] = +0.49$), because of the high metallicity the dust-to-gas ratio measured in this system ($\log \kappa = -0.8$) is similar to that of other systems in which H_2 is detected (see Fig. 15 of Ledoux et al. 2003). Substantial star-formation activity must have taken place in the past history of this DLA system. Note that the age of the Universe at $z = 4.22$ is 1.5 Gyr (for $\Omega_{\Lambda} = 0.73$, $\Omega_{\text{m}} = 0.27$ and $H_0 = 71 \text{ km s}^{-1} \text{ Mpc}^{-1}$).

Nitrogen is thought to have both primary and secondary origins depending on whether the seed carbon and oxygen nuclei are produced by the star itself or are already present in the ISM from which the star formed. In the case of secondary nitrogen production, the ratio of nitrogen to oxygen abundances increases with increasing oxygen abundance, whereas for primary production this ratio remains constant and nitrogen tracks oxygen (this is the

so-called primary plateau). In the low-metallicity H II regions of nearby galaxies, $[N/O]$ abundance ratios tend to lie around the primary plateau (with $[N/O] = -0.73 \pm 0.13$) for $[O/H] < -1$, and have a secondary behaviour for $[O/H] > -1$ (van Zee et al. 1998; Izotov & Thuan 1999). Similarly, most DLA systems show a plateau at $[N/O] \approx -0.9$ (see Centuri3n et al. 2003; Pettini et al. 2002). The abundance of nitrogen relative to sulfur at $z_{\text{abs}} = 4.224$ toward PSS J1443+2724, $[N/S] = -0.75$, corresponds exactly to the primary nitrogen production plateau (assuming $[O/S] = 0$). If we assume the widely accepted hypothesis that primary nitrogen is produced in intermediate-mass stars ($4 \leq M_{\odot} \leq 8$) during the Asymptotic Giant Branch phase (Henry et al. 2000), then star-formation activity must have started in this system at least $2 - 5 \times 10^8$ yrs before $z = 4.224$ accounting for the characteristic lag time for intermediate-mass stars to eject nitrogen. This is similar to what is observed in the $z_{\text{abs}} = 4.383$ system toward BRI 1202–0725 (D’Odorico & Molaro 2004).

Argon can be ionised in H I regions and is therefore a tracer of the radiation field. In the presently studied system, we find $[Ar/S] = -0.30$, which is higher than in most other DLA systems (Vladilo et al. 2003). This is consistent with the associated galaxy being in a quiescent state at the time of observation, as also inferred below from the analysis of H₂ lines.

3.2. Molecular hydrogen

The H₂ transitions are numerous and the spectral resolution of our data is high enough to allow unambiguous detection and detailed analysis of H₂ (see Fig. 1). Great care has been exercised when fitting the absorption lines with multi-component Voigt profiles. H₂ is detected in four different rotational levels ($J = 0, 1, 2$ and 3) of the vibrational ground-state in three velocity components with total column densities of $\log N(\text{H}_2) = 17.67, 17.97, 17.48$ and 17.26 respectively (see Tables 1 and 2). The $J = 4$ level is tentatively detected in the strongest component with $\log N(\text{H}_2) \sim 14$. Blending is heavy however and this could be an upper limit. The detection of H₂ confirms the previous claim that most of the gas in this DLA system is cold (Howk et al. 2005). The total H₂ column density is one of the largest observed in DLA systems and the molecular fraction is $\log f = -2.38 \pm 0.13$, with $f = 2N(\text{H}_2)/(2N(\text{H}_2) + N(\text{H I}))$. HD is not detected down to 3σ limits of $\log N(\text{HD}) < 13.6$ and 13.7 for $J = 0$ and 1 respectively, implying that $[\text{HD}/\text{H}_2] < -4.2$.

The excitation temperatures T_{01} for the two main components of the system are 96 and 136 K respectively (see Table 2). The excitation temperatures for higher rotational levels are slightly larger, possibly as a consequence of the levels being populated by radiative or

formation pumping. By equating H_2 formation and destruction rates, we write:

$$SIn(\text{H}_2) = Rn(\text{H})n \quad (1)$$

where $n = n(\text{H}) + 2n(\text{H}_2)$ is the particle density, I is the H_2 dissociation rate in the unshielded UV background (in s^{-1}) and $S = [N(\text{H}_2)/10^{14} \text{ cm}^{-2}]^{-0.75}$ is the correction factor for shielding (Draine & Bertoldi 1996; Hirashita & Ferrara 2005). $R = 4.1 \times 10^{-17} [T/10^2 \text{ K}]^{0.5} (Z/Z_\odot) D \text{ cm}^3 \text{ s}^{-1}$ is the H_2 formation rate per unit volume and time, $Z/Z_\odot = 0.23$ is the metallicity relative to Solar and $D = 0.7$ is the fraction of metals into dust.

The H_2 $J = 4$ level is mostly populated by pumping of lower rotational levels by absorption of UV photons from the ambient radiation field and subsequent radiative cascade, and by direct formation of the molecule in this excited state. Following the simple procedure introduced by Jura (1975), we write the equation describing the equilibrium of the $J = 4$ level population as:

$$9.1p_{4,0}SIn(\text{H}_2, J = 0) + 0.19Rn(\text{H})n = A(4 \rightarrow 2)n(\text{H}_2, J = 4) \quad (2)$$

where $p_{4,0} = 0.26$ is the pumping efficiency into the $J = 4$ level from the $J = 0$ level and $A(4 \rightarrow 2) = 2.8 \times 10^{-9} \text{ s}^{-1}$ denotes the spontaneous transition probability from $J = 4$ to $J = 2$.

Combining the above equations and using the total column densities given in Table 1, we find $Rn = 4 \times 10^{-16} \text{ s}^{-1}$. This is probably an upper limit given the possibility that $N(J = 4)$ be an upper limit. Assuming a temperature of $T = 150 \text{ K}$, we derive a density of $n_{\text{H}} \leq 50 \text{ cm}^{-3}$. This value could be slightly larger in case of any α -element enhancement. The corresponding H_2 dissociation rate is $I \leq 3 \times 10^{-10} \text{ s}^{-1}$. This is of the order of or smaller than the highly variable photo-dissociation rate observed in the ISM of the Galaxy (e.g., Hirashita & Ferrara 2005). This probably indicates, as expected above, that there is little on-going star formation in the galaxy associated with this DLA system. This is consistent with the fact that no emitting counterpart has been found using the Lyman-break techniques down to $L \sim L_{\text{LBG}}^*/4$ (Prochaska et al. 2002) or in Lyman- α emission down to $2 \times 10^{-17} \text{ erg cm}^{-2} \text{ s}^{-1}$ from 2D-spectroscopy at the Canada-France-Hawaii Telescope (Ledoux 1999).

3.3. The Cosmic Microwave Background temperature

Absorption lines from the ground-state and first fine-structure excited level of C I are detected (see Fig. 2) at redshifts of $z_{\text{abs}} = 4.22379$ and 4.22413 , slightly larger than those of the molecular components. The Doppler parameters are larger as well indicating that the C I gas spans a slightly larger velocity range than the H_2 gas (see also Ledoux et al. 2003). We

measure $[\text{C I}^*/\text{C I}] = -0.09 \pm 0.05$ and -0.21 ± 0.04 in each of the two components respectively. This is surprisingly small at high redshift. Indeed, the value expected for excitation by the Cosmic Microwave Background Radiation (CMBR) field alone, with a temperature of 14.2 K at $z = 4.22$, is -0.15 (Silva & Viegas 2002). In addition, part of the excitation can be due to UV or IR pumping although this is probably negligible here. In Fig. 3, we plot the expected values for $[\text{C I}^*/\text{C I}]$ as a function of temperature of the cold gas. The first C I component has a density ($n_{\text{H}} \leq 25 \text{ cm}^{-3}$) that is similar to what is measured in the H_2 gas and is thus probably predominantly associated with it. The second C I component probably has a lower density and the corresponding $[\text{C I}^*/\text{C I}]$ ratio is consistent with what is expected for excitation by the CMBR field alone.

4. Conclusion

The direct detection of H_2 at high redshift is a unique tool for studying the ISM in the remote Universe. We have detected molecular hydrogen in one of the highest redshift DLA systems known to date ($z_{\text{abs}} = 4.224$). We have shown that the gas is probably the left-over of intense star-formation activity that happened at least 2×10^8 yrs before the time of observation and that the associated object is in a quiescent phase. The UV radiation field is of the order of or smaller than that in the Galaxy and the gas is cold ($T \sim 90 - 180$ K). The $[\text{C I}^*/\text{C I}]$ ratio in one of the components of the system is consistent with what is expected for excitation by the CMBR field at this redshift ($T = 14.2$ K). This study demonstrates the importance of this kind of observations for our understanding of how star formation proceeds at high redshift. The prospect of using γ -ray burst afterglows as background sources for similar studies is exciting and will boost this field in a near future (Draine & Hao 2002).

This work is based on data collected under prog. 072.A-0346 of the European Southern Observatory with UVES mounted on the 8.2 m Kueyen telescope at the Paranal Observatory, Chile. We thank the referee, Paolo Molaro, for fruitful comments. PP and RS acknowledge support from the Indo-French Centre for the Promotion of Advanced Research (Centre Franco-Indien pour la Promotion de la Recherche Avancée) under contract No. 3004-3.

REFERENCES

- Ballester, P., Modigliani, A., Boitquin, O., Cristiani, S., Hanuschik, R., Kaufer, A., & Wolf, S. 2000, *The Messenger*, 101, 31

- Centurión, M., Molaro, P., Vladilo, G., Péroux, C., Levshakov, S. A., & D’Odorico, V. 2003, *A&A*, 403, 55
- Cui, J., Bechtold, J., Ge, J., & Meyer, D. M. 2005, *ApJ*, 633, 649
- Dekker, H., D’Odorico, S., Kaufer, A., Delabre, B., & Kotzlowski, H. 2000, *Proc. SPIE*, 4008, 534
- D’Odorico, V., & Molaro, P. 2004, *A&A*, 415, 879
- Draine, B. T., & Bertoldi, F. 1996, *ApJ*, 468, 269
- Draine, B. T., & Hao, L. 2002, *ApJ*, 569, 780
- Ge, J., & Bechtold, J. 1999, in *Highly Redshifted Radio Lines*, Carilli, C. L., et al., eds., ASP Conf. Ser. 156, 121
- Grevesse, N., & Sauval, A. J. 2002, *Adv. Space Res.*, 30, 3
- Henry, R. B. C., Edmunds, M. G., & Köppen, J. 2000, *ApJ*, 541, 660
- Hirashita, H., & Ferrara, A. 2005, *MNRAS*, 356, 1529
- Howk, J. C., Wolfe, A. M., & Prochaska, J. X. 2005, *ApJ*, 622, L81
- Izotov, Y. I., & Thuan, T. X. 1999, *ApJ*, 511, 639
- Jura, M. 1975, *ApJ*, 197, 581
- Ledoux, C. 1999, Ph.D. Thesis
- Ledoux, C., Srianand, R., & Petitjean, P. 2002, *A&A*, 392, 781
- Ledoux, C., Petitjean, P., & Srianand, R. 2003, *MNRAS*, 346, 209
- Levshakov, S. A., & Varshalovich, D. A. 1985, *MNRAS*, 212, 517
- Levshakov, S. A., Dessauges-Zavadsky, M., D’Odorico, S., & Molaro, P. 2002, *ApJ*, 565, 696
- Omont, A., Petitjean, P., Guilloteau, S., McMahon, R. G., Solomon, P. M., & Pécontal, E. 1996, *Nature*, 382, 428
- Petitjean, P., Srianand, R., & Ledoux, C. 2000, *A&A*, 364, L26
- Pettini, M., Ellison, S. L., Bergeron, J., & Petitjean, P. 2002, *A&A*, 391, 21

Prochaska, J. X., et al. 2001, ApJS, 137, 21

Prochaska, J. X., Gawiser, E., Wolfe, A. M., Quirrenbach, A., Lanzetta, K. M., Chen, H.-W.,
Cooke, J., & Yahata, N. 2002, AJ, 123, 2206

Prochaska, J. X., Gawiser, E., Wolfe, A. M., Castro, S., & Djorgovski, S. G. 2003, ApJ, 595,
L9

Silva, A. I., & Viegas, S. M. 2002, MNRAS, 329, 135

Solomon, P. M., & Vanden Bout, P. A. 2005, ARA&A, 43, 677

Vladilo, G., Centurión, M., D’Odorico, V., & Péroux, C. 2003, A&A, 402, 487

van Zee, L., Salzer, J. J., Haynes, M. P., O’Donoghue, A. A., & Balonek, T. J. 1998, AJ,
116, 2805

Table 1: Total column densities of different species in the DLA system at $z_{\text{abs}} = 4.224$ toward PSS J 1443+2724

Species	Transition lines	$\log N \pm \sigma_{\log N}$	Metallicity relative to Solar ^a
H I	1025,1215	20.95 ± 0.10	...
H ₂	J=0 lines	17.67 ± 0.06	...
H ₂	J=1 lines	17.97 ± 0.05	...
H ₂	J=2 lines	17.48 ± 0.12	...
H ₂	J=3 lines	17.26 ± 0.17	...
H ₂	J=4 lines	14.02 ± 0.14	...
C I	1277,1280	13.12 ± 0.02	...
C I*	1277,1279	12.97 ± 0.03	...
C I**	1277,1280	≤ 12.5	...
N I	953.4,1134.1	15.52 ± 0.01	-1.38 ± 0.10
Mg II	1239,1240	15.98 ± 0.01	-0.55 ± 0.10
S II	1250	15.52 ± 0.01	-0.63 ± 0.10
Ar I	1066	14.42 ± 0.01	-0.93 ± 0.10
Fe II	1081	15.33 ± 0.03	-1.12 ± 0.10

^a Solar abundances adopted from Grevesse & Sauval (2002).

Note: errors in the column densities of metals correspond to the rms errors from fitting the Voigt profiles. They do not include the uncertainties related to the continuum placement.

Table 2: Column densities and excitation temperatures from Voigt-profile fitting of H₂ molecular lines

z_{abs}	Level	$\log N$ $\pm \sigma_{\log N}$	$b \pm \sigma_b$ [km s ⁻¹]	T_{ex} [K]	J_{ex}
4.22371	J=0	17.41 ^{+0.02} _{-0.05}	0.8 ± 0.3
	J=1	17.59 ^{+0.03} _{-0.03}	”	90-107	0-1
	J=2	17.15 ^{+0.05} _{-0.13}	”	200-259	0-2
	J=3	16.53 ^{+0.17} _{-0.91}	”	156-302	1-3
	J=4	< 13.6 ^a	”
4.22401	J=0	17.34 ^{+0.09} _{-0.07}	1.1 ± 0.3
	J=1	17.75 ^{+0.06} _{-0.08}	”	104-179	0-1
	J=2	17.25 ^{+0.13} _{-0.14}	”	218-377	0-2
	J=3	17.21 ^{+0.13} _{-0.13}	”	337-530	1-3
	J=4	14.02 ^{+0.15} _{-0.07}	”
4.22416	J=0	14.34 ^{+0.00} _{-0.12}	1.7 ± 0.5
	J=1	14.86 ^{+0.04} _{-0.13}	”
	J=2	14.61 ^{+0.06} _{-0.15}	”
	J=3	14.18 ^{+0.00} _{-0.16}	”
	J=4	< 13.6 ^a	”

^a 3 σ detection limit.

Note: errors in the column densities correspond to the range $b \pm \sigma_b$ of Doppler parameters and not to the rms errors from fitting the Voigt profiles.

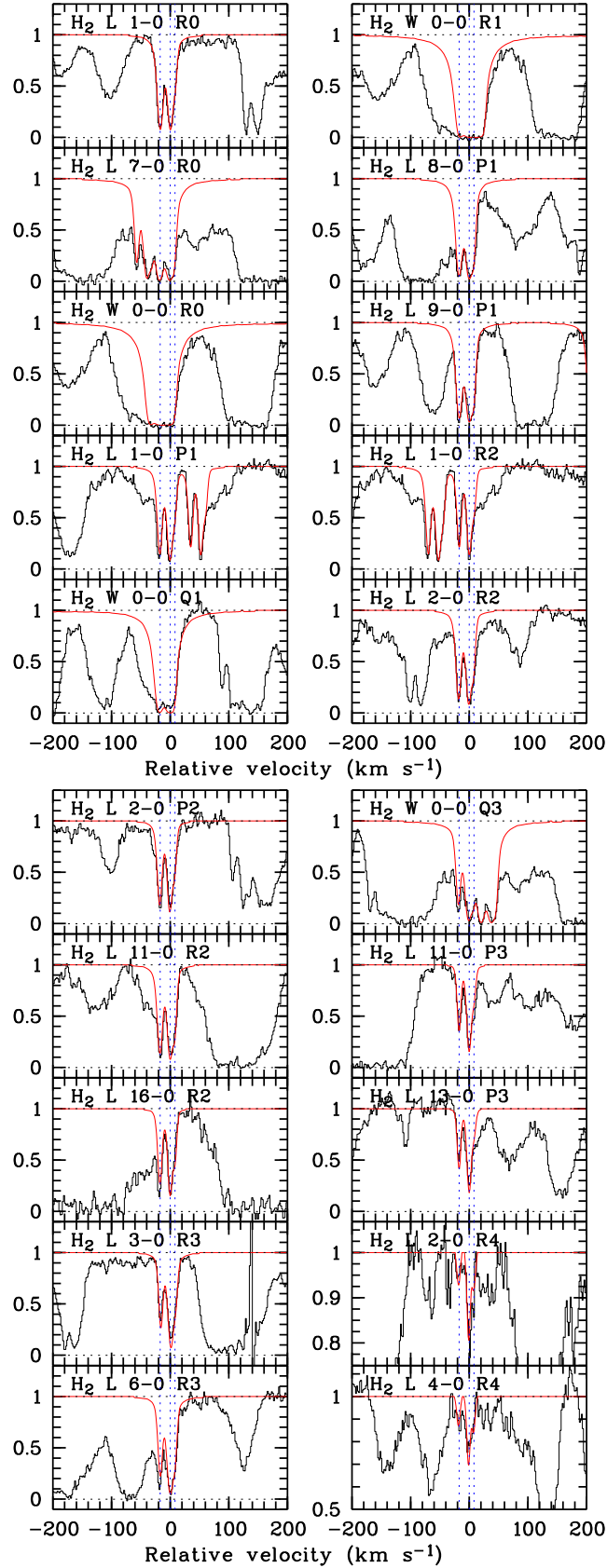


Fig. 1.— Velocity profiles of selected transition lines from the $J = 0, 1, 2, 3$ and 4 rotational levels of the vibrational ground-state Lyman and Werner bands of H_2 at $z_{\text{abs}} = 4.224$ toward DCS J1443+2724. The plot shows the observed flux (black line) and the model fit (red line). The vertical dashed blue line indicates the rest-frame Lyman- α emission line.

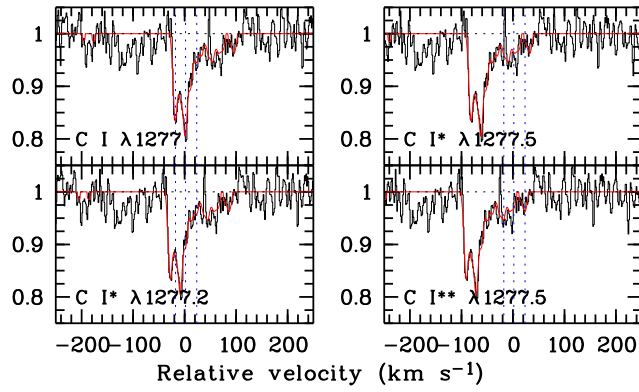


Fig. 2.— Velocity profiles of C I and C I* transition lines at $z_{\text{abs}} = 4.22379$ and 4.22413 toward PSS J1443+2724. The best Voigt-profile fit is superposed on the observed spectrum with vertical dotted lines marking the location of the two detected components of the system and a third, possible component.

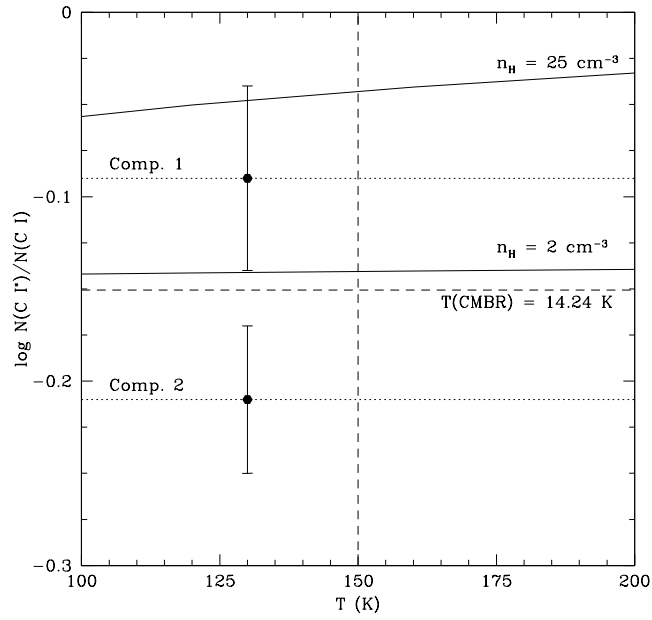


Fig. 3.— $[\text{C I}^*/\text{C I}]$ ratio versus temperature. Filled circles with error bars are the measurements in the $z_{\text{abs}} = 4.22379$ and 4.22413 components toward PSS J 1443+2724. LTE predictions for two different values of the particle density are shown by solid lines. The value expected for excitation by the CMBR field alone is shown by the horizontal long-dashed line.